

Inertial Sensor Based Motion Trajectory Visualization and Quantitative Quality Assessment of Hemiparetic Gait

Yan Wang, James Xu, Xiaoyu Xu, Xiaoxu Wu, Gregory Pottie and William Kasier
Department of Electrical Engineering, University of California, Los Angeles
{phylliswany, jyxu, x2y, xiaoxuwu}@ucla.edu, {pottie, kaiser}@ee.ucla.edu

ABSTRACT

The analysis of the biomechanics surrounding human gait has been used by many disciplines, and is especially useful in fields such as neurology, where many diseases are diagnosed clinically through careful observations of a person's movement. In patients afflicted by neurological diseases, hemiparetic gait is common and this abnormal gait causes the state of the art in motion reconstruction to fail. This paper presents two novel contributions to the area. The first is a novel gait trajectory reconstruction and visualization method with a zero velocity detection method targeting hemiparetic gait patterns, enabling reconstruction and visualization of hemiparetic gait in true 3D space. The second is a set of novel quality metrics developed in conjunction with the UCLA Department of Neurology, for evaluating patients suffering from neurological diseases.

1. INTRODUCTION

The analysis of the biomechanics surrounding human gait has been used by many disciplines to measure quality of movements, diagnose diseases and guide rehabilitation efforts. It is especially useful in fields such as neurology, where many diseases are diagnosed clinically through careful observations of a person's movement using either gait laboratories or standard tests. For America's afflicted groups such as the 1.5 million currently suffering from Parkinson's disease or the 795,000 stroke patients, the monitoring and characterization of gait parameters both at a clinic and in-community is essential for improving diagnoses, guiding treatment and providing at-home physical rehabilitation [1, 3].

Due to the important benefits demonstrated by the monitoring and analysis of gait characteristics, a number of methods have been proposed that aim to track the foot during a gait cycle and to characterize the cycle using various metrics. In [5], wireless inertial sensors containing accelerometers, gyroscopes and magnetometers were used to determine the foot motion in 3D space. The study used a straightforward zero velocity update (ZUPT) method to determine reset points for integration when a foot becomes stationary.

Another system for visualizing gait was introduced in [6], following a similar approach to [5] in terms of 3D position tracking, but with the addition of two shoe mounted force sensors to both augment trajectory data with the force of the foot and to detect the various phases of gait for resetting integration. Various features that characterize a gait cycle is studied in [2], the study presented a way to reconstruct a foot's movement in the sagittal plane using 2D accelerometer combined with 1D gyroscope. Based on this data, stride length, walking speed, gait phase timing and incline were estimated. While much previous work demonstrated methods to reconstruct gait cycles, these methods contain major short comings for use in the clinical setting to study hemiparetic gait exhibited by patients suffering from neurological diseases: 1). Many are focused on reconstructing motions on the sagittal plane, which is not sufficient as hemiparetic gait can exhibit large swings in both transverse and coronal planes; 2). Most previous works do not consider the problem of accurately detecting a correct reset point for ZUPT. The weak side of a hemiparetic patient produces irregular gait patterns causing most zero velocity detection algorithms (and thus the reconstruction algorithms) to fail; 3). There are a limited number of clinically meaningful features extracted to characterize abnormal (hemiparetic) gait.

In solving these challenges, this paper presents both a novel gait trajectory reconstruction and visualization method with a zero velocity detection algorithm targeting hemiparetic gait patterns, and a set of novel gait quality metrics that can be extracted from the motion trajectory.

2. DATA COLLECTION SYSTEM

Two InvenSense Motion SDK sensors were mounted on both shoes by Velcro to collect walking data (Figure 1). Sensors were sampled at 200Hz and the output data include raw accelerometer measurements, gyroscope measurements and filtered sensor orientation (in quaternions). Data were transmitted through the on-board Bluetooth to a local PC and partially synchronized according to the receiving time. In addition, foot hopping was also required to generate motion signatures for further synchronization.



Figure 1: Sensor mounting position on the shoe.

Permission to make digital or hard copies of all or part of this work for personal or classroom use is granted without fee provided that copies are not made or distributed for profit or commercial advantage and that copies bear this notice and the full citation on the first page. To copy otherwise, to republish, to post on servers or to redistribute to lists, requires prior specific permission and/or a fee.

BODYNETS 2013, September 30-October 02, Boston, United States

Copyright © 2013 ICST 978-1-936968-89-3

DOI 10.4108/icst.bodynets.2013.253556

3. MOTION TRACKING OF HEMIPARETIC WALKING

The signal processing system tracks foot motions and projects motion trajectories into a visualization frame.

3.1 Motion Tracking Algorithm

The strapdown inertial navigation algorithm [8] is applied to track foot motions using the orientation output by the sensor. To eliminate the drift in position estimation, ZUPT is used [4] so that windows need to be correctly detected when the foot is stationary. A detection method similar to the Acceleration Magnitude Detector [7] is applied. First, the acceleration signal in the global frame was stripped of the gravity component. Then, the mean of the pure acceleration energy within a sliding window (0.1s in our analysis) is evaluated. By selecting a proper threshold ($0.025\text{m}^2/\text{s}^4$ in our analysis), this method is effective for detecting windows of zero velocity among normal gaits. However, since hemiparetic subjects usually present much weaker strides on the afflicted leg, false positives are unavoidable and common.

Analysis on a set of videotaped hemiparetic walks indicates that due to the weakness of the afflicted leg, it is not able to support the body weight and so the step of that side is weaker compared to the healthy side. Based on this observation, we introduce a new zero velocity detection method. First, a threshold is applied to the healthy side to determine the zero velocity windows for that side. Second, the motion windows (signals between two neighboring zero velocity windows) are mapped to the afflicted side as the zero velocity windows. Third, adjustment of the zero velocity windows of the afflicted side is performed through window appending (including the starting and ending parts of the signal where both feet were stationary), shifting (reducing the effect of sensor synchronization issues), expanding (including the parts where double support occurred), and shrinking (excluding the samples with high acceleration energy at the window boundaries). As the zero velocity window detection of the afflicted side relies on that of the healthy side, the best detection accuracy need to be obtained for the latter. Here proper window merging (reducing false negatives) and splitting (reducing false positives) are added to enhanced the detection on the healthy side. For merging, the average length of the motion windows is calculated. Each individual window with length smaller than half of the averaged length is removed by merging its two neighboring zero velocity windows together. For splitting, the average length of the updated zero velocity windows is calculated again and if the length of an individual window is larger than twice the average then tighter thresholds are used for thresholding within the current window so that it can be split up. Figure 2 illustrates an example zero velocity window detection result on a hemiparetic walking set.

Successful implementation of the above procedure requires the prior knowledge of which leg is the afflicted side. To automate this labeling step, the maximum magnitude of the power spectral density of the y-axis gravity-removed acceleration signal in the global frame is estimated for both sides, and the ratio of the left side over the right is calculated. Compared to healthy subjects with balanced gait, hemiparetic subjects have significant disparities of walking strengths between the two sides, thus the ratio can infer whether a dataset is a hemiparetic walking set and if so

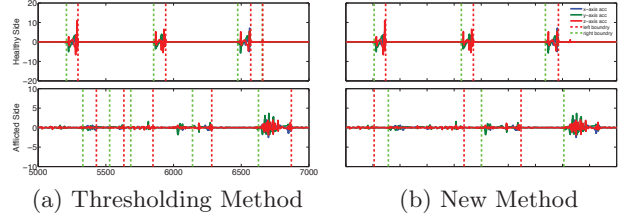


Figure 2: Improvements on the zero velocity window detection of hemiparetic walking by introducing the new method.

which leg is hemiparetic.

3.2 Reconstruction of Foot Trajectory

A 6DOF sensor is unable to precisely determine its orientation in the North-East-Down coordinate system due to the lack of a magnetometer. However for visualization and analysis it is essential to project the left and right foot motion trajectories of multiple experiments into the same frame of reference. Perfectly aligning the sensor frames with a fixed global coordinate system initially for each dataset is feasible but highly inconvenient in clinical applications. To address this challenge, we introduce a new visualization frame that is determined by walking direction and gravity.

Before walking, subjects were asked to stay stationary for 1 second to construct the initialization frame (the global frame mentioned in the previous sections). During this period, the mean of the accelerometer signal, \mathbf{a}_0 , and the mean of the filtered quaternion, \mathbf{q}_0 , are calculated. \mathbf{a}_0 is a measurement of the gravity in the initialization frame. By taking quaternion division of \mathbf{q} over \mathbf{q}_0 , the result \mathbf{q}^0 represents the sensor orientation in the initialization frame. \mathbf{a}_0 and \mathbf{q}_0 enable foot motion tracking in the initialization frame.

The motion tracking algorithm estimates the foot position \mathbf{p}^0 in the initialization frame. For each data set, walking is precluded and concluded by a zero velocity window. Centers of the two zero velocity windows i_s and i_e signify the starting and ending of the walk. By subtracting the starting foot position $\mathbf{p}_{i_s}^0$ from the ending position $\mathbf{p}_{i_e}^0$, the resulting vector \mathbf{v}_d^0 represents the walking direction in the initialization frame. Then, x^0 , y^0 and z^0 , the base of the visualization frame, can be constructed,

$$\begin{aligned} \mathbf{z}^0 &= \mathbf{a}_0 / \|\mathbf{a}_0\|, \\ \mathbf{x}^0 &= (-\mathbf{v}_d^0 / \|\mathbf{v}_d^0\|) \times \mathbf{z}, \\ \mathbf{y}^0 &= (\mathbf{z} \times \mathbf{x}) / \|\mathbf{z} \times \mathbf{x}\|. \end{aligned}$$

By putting the column vector \mathbf{x}^0 , \mathbf{y}^0 and \mathbf{z}^0 together as a 3×3 matrix B_v^0 , the rotation matrix R_0^v presenting the orientation of the visualization frame relative to the initialization frame can be calculated as,

$$R_0^v = (B_v^0)^{-1}.$$

Therefore, for an arbitrary position \mathbf{p}^0 in the initialization frame, it can be projected onto the visualization frame as \mathbf{p}^v through the following multiplication,

$$\mathbf{p}^v = R_0^v \cdot \mathbf{p}^0.$$

Since \mathbf{x}^0 is perpendicular to the walking direction, the foot deviation from the walking direction is observable. Also,

since \mathbf{z}^0 is defined by gravity, level walking, stair ascending and descending are discernible. Due to the individual sensor offsets, using the gravity component of the accelerometer measurements will lead to small misalignments of the left and right visualization frames. However the precision is sufficient for visualization purpose.

4. EVALUATION METRICS EXTRACTION

The parameters of clinical interest not only include direct parameters such as walking speed (WS), individual stride length (SL), foot swing time (SwingT) and stance time (StanceT), but also include derived metrics such as stride-to-stride variation, maximum foot front deviating distance (MDD), maximum foot front lifting height (MLH) and maximum heel lifting rotation angle (MLR). As our method is able to measure foot orientation and position in 3D space, all of the above features are exactable for detailed gait characterization.

4.1 Direct Parameters

Besides the centers of the starting and ending zero velocity windows, we label the centers of the remaining zero velocity windows where stance occurs as $i_k, k = 1, 2, \dots, N$. By converting i_s and i_e to i_0 and i_{N+1} ,

$$WS = \|\mathbf{p}_{i_{N+1}}^v - \mathbf{p}_{i_0}^v\| / [(i_{N+1} - i_0) \cdot SR], SR = 1/200,$$

$$SL(k) = \|\mathbf{p}_{i_{k+1}}^v - \mathbf{p}_{i_k}^v\|, k = 0, 1, 2, \dots, N.$$

To determine stance phase and swing phase of normal gaits, which are separated by toeff and heelstrike, peak detection algorithm can be applied to the gyroscope signal [2]. However, hemiparetic subjects typically present difficulties in performing toeff and heelstrike on the afflicted side. Instead, they can be seen dragging the hemiparetic limbs with the front of the toe constantly touching the ground. Thus, in our analysis, stance phase is approximated by zero velocity windows while swing phase is approximated by motion windows,

$$StanceT(k) = (r_k - l_k) \cdot SR, \quad k = 1, 2, 3, \dots, N,$$

$$SwingT(k) = (l_{k+1} - r_k) \cdot SR, \quad k = 0, 1, 2, \dots, N,$$

where l_k and r_k are the indexes of the left and right boundary of the k th zero velocity window.

4.2 Derived Parameters

Strides are segmented at the center of zero velocity windows. To quantitatively assess the stride-to-stride variation, they are further projected into individual local frames where the position and orientation of the first sample are set to be zero. Dynamic Time Warping (DTW) is applied to stretch two neighboring strides from the same side to the same length based on the signal waveform along the new y axis (Figure 3). To avoid the effect of amplitude on the stretching algorithm, the data are normalized to the interval between 0 and 1. Then, the position variation (PV), and orientation variation (OV) can be calculated,

$$PV(k) = \sqrt{\frac{\sum_{i=1}^{l_{k,k+1}} (\mathbf{pos}_{k+1}(i) - \mathbf{pos}_k(i))^2}{l_{k,k+1}}},$$

$$OV(k) = \sqrt{\frac{\sum_{i=1}^{l_{k,k+1}} (\mathbf{ori}_{k+1}(i) - \mathbf{ori}_k(i))^2}{l_{k,k+1}}}, k = 0, 1, 2, \dots, N - 1,$$

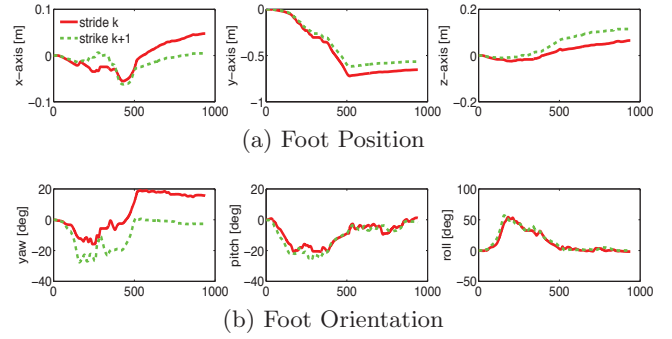


Figure 3: Two stretched neighboring strides in their local frames after applying DTW.

where $\mathbf{pos}_k(i)$ and $\mathbf{ori}_k(i)$ represent the foot position and orientation at the index i of the k th stretched stride and $l_{k,k+1}$ represents the length of that stretched stride. Similarly, other parameters are also calculated within each stride in its local frame,

$$MDD(k) = \max_i \|\mathit{pos}_k(i)\|,$$

$$MLH(k) = \max_i \mathit{pos}_k(i),$$

$$MLR(k) = \max_i \mathit{yaw}_k(i), k = 0, 1, 2, \dots, N, i = 1, 2, 3, \dots, l_k,$$

where $\mathit{pos}_k(i)$, $\mathit{pos}_k(i)$, and $\mathit{yaw}_k(i)$ are the foot position along the local x axis, z axis, and foot rotation along the z axis respectively. l_k is the length of the stride before stretching.

5. EXPERIMENTAL RESULTS

The validation process is performed in two parts. First, to validate the motion tracking algorithm, three healthy subjects were recruited and each performed two sets of 40-meter level walking, 10-step stair ascending, and 10-step stair descending. The absolute error of the distance estimation across the left and right sides is $(3.08 \pm 1.77)\%$. Foot position and orientation waveforms of individual steps are compared with the Vicon captured data from the CMU Graphics Lab Motion Capture Database. Though the data were collected from different subjects, normal gaits usually present uniform patterns. Figure 4 illustrates the capability of the trajectory reconstruction algorithm to differentiate stair climbing and level walking.

Second, to test the system on hemiparetic gait, a staff member from the UCLA Neurological Rehabilitation & Research Unit working closely with post-stroke patients was asked to mimic the top five most common hemiparetic gaits through 10-meter level walking (a standard clinical test). The absolute error of distance estimation from the healthy side is $(1.01 \pm 0.72)\%$ while that from the hemiparetic side is $(3.55 \pm 3.60)\%$. To verify the effectiveness of the evaluation metrics, a set of normal 10-meter walks was also collected as the control group. Figure 5 illustrates the 3D visualization of the mean and standard deviation of the strides collected

Table 1: Walking Speed (Hi = Hemiparetic i).

	Control(C)	H1	H2	H3	H4	H5
S[m/s]	1.06	0.30	0.28	0.28	0.21	0.25

Table 2: Parameters to Characterize Gaits (H = Healthy, A = Afflicted).

	Side	SL[m]	SwingT[s]	StanceT[s]	PV[m]	OV[deg]	MDD[m]	MHL[m]	MLR[deg]
C	H	1.37 ± 0.06	0.61 ± 0.02	0.51 ± 0.06	0.07 ± 0.02	7.42 ± 1.65	0.02 ± 0.03	0.14 ± 0.01	61.21 ± 1.13
	H	1.38 ± 0.06	0.60 ± 0.02	0.50 ± 0.03	0.06 ± 0.04	4.31 ± 1.17	0.07 ± 0.05	0.17 ± 0.02	64.08 ± 1.78
H1	A	0.83 ± 0.08	1.54 ± 0.25	1.04 ± 0.40	0.10 ± 0.04	10.63 ± 4.76	0.02 ± 0.03	0.04 ± 0.01	44.03 ± 9.90
	H	0.85 ± 0.06	0.44 ± 0.04	2.05 ± 0.21	0.14 ± 0.10	6.99 ± 3.32	0.04 ± 0.03	0.26 ± 0.16	64.79 ± 2.93
H2	A	0.79 ± 0.07	1.95 ± 0.23	0.76 ± 0.24	0.09 ± 0.05	11.87 ± 4.61	0.02 ± 0.03	0.03 ± 0.02	62.45 ± 4.79
	H	0.79 ± 0.05	0.47 ± 0.04	2.19 ± 0.21	0.08 ± 0.03	6.18 ± 2.06	0.03 ± 0.03	0.12 ± 0.05	54.38 ± 6.06
H3	A	0.71 ± 0.27	1.22 ± 0.32	1.07 ± 0.33	0.43 ± 0.17	68.05 ± 29.82	0.08 ± 0.13	0.03 ± 0.02	22.66 ± 8.85
	H	0.72 ± 0.10	0.46 ± 0.06	1.83 ± 0.21	0.21 ± 0.07	28.65 ± 17.12	0.07 ± 0.10	0.15 ± 0.10	50.57 ± 9.15
H4	A	0.72 ± 0.11	2.37 ± 0.55	0.98 ± 0.41	0.08 ± 0.03	15.12 ± 6.97	0.02 ± 0.03	0.08 ± 0.03	49.80 ± 8.47
	H	0.75 ± 0.09	0.46 ± 0.04	2.83 ± 0.27	0.10 ± 0.06	7.30 ± 2.52	0.03 ± 0.03	0.15 ± 0.10	40.24 ± 10.25
H5	A	0.66 ± 0.08	1.39 ± 0.18	1.11 ± 0.37	0.07 ± 0.04	10.81 ± 4.30	0.01 ± 0.02	0.03 ± 0.01	31.42 ± 10.47
	H	0.69 ± 0.06	0.43 ± 0.04	2.03 ± 0.14	0.11 ± 0.08	8.36 ± 3.09	0.03 ± 0.03	0.13 ± 0.11	57.39 ± 7.19

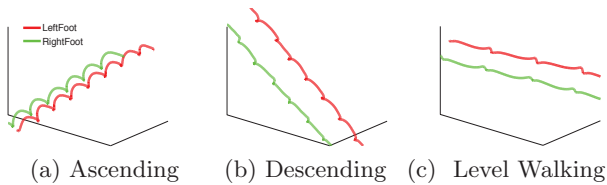


Figure 4: Foot trajectory reconstruction for visualization.

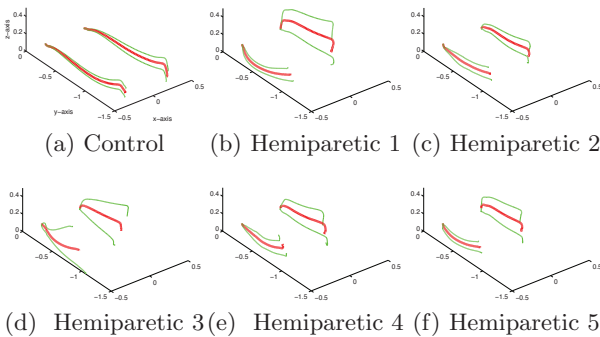


Figure 5: 3D visualization of strides collected from different gaits. The center red line indicates the mean while the green line indicates the mean plus standard deviation and mean minus standard deviation.

from different gaits where strides belonging to the same group are stretched to the same length (The first and last strides have been truncated since some of them do not have a complete swing phase). Table 1 summarizes the average walking speed calculated from the left and right foot sensors and Table 2 lists the rest of the gait quality related parameters. For most of the parameters, the difference between normal and the hemiparetic gaits is easily observable, especially by comparing the symmetry of the two sides. Though $StanceT(k)$ and $SwingT(k)$ defined in the paper are approximations to the swing time and stance time defined in clinic, they are good indicators of gait symmetry temporally. The only exception is MDD due to its small magnitude that can be easily disturbed through frame projection.

6. CONCLUSIONS

This paper presented both a novel gait trajectory reconstruction and visualization method with a zero velocity detection algorithm targeting hemiparetic gait patterns, and a set of novel quality metrics that can be quantified based on the motion trajectory. Through initial experimental data, we demonstrated that: first, the motion tracking algorithm produce sufficient estimation accuracy for gait analysis; second, the trajectory projection algorithm is able to differentiate many types of walking such as level walking and stair climbing; finally, many parameters can be extracted from the trajectory to form metrics that are clinically useful in evaluating patients suffering from neurological diseases.

7. REFERENCES

- [1] B. H. Dobkin and A. Dorsch. The promise of mhealth: Daily activity monitoring and outcome assessment by wearable sensors. *Neurorehabilitation and Neural Repair*, 25:788–798.
- [2] S. A. M. C. S. S. C. F. Assessment of walking features from foot inertial sensing. *IEEE Transactions on Biomedical Engineering*, 52:486–494, 2005.
- [3] M. F. Gordon. Physical activity and exercise recommendations for stroke survivors. *Stroke*, pages 1230–1240, 2004.
- [4] A. Jimenez, F. Seco, C. Prieto, and J. Guevara. A comparison of pedestrian dead-reckoning algorithms using a low-cost mems imu. In *Intelligent Signal Processing, 2009. WISP 2009. IEEE International Symposium on*, pages 37–42, 2009.
- [5] T. I. G. S. B. R. G. D. A. M. J. Results of using a wireless inertial measuring system to quantify gait motions in control subjects. *IEEE Transactions on Information Technology in Biomedicine*, pages 904–915, 2010.
- [6] S. H. K. H. F. J. M. V. P. H. Ambulatory assessment of ankle and foot dynamics. *IEEE Transactions on Biomedical Engineering*, 54:895–902, 2007.
- [7] I. Skog, J.-O. Nilsson, and P. Handel. Evaluation of zero-velocity detectors for foot-mounted inertial navigation systems. In *Indoor Positioning and Indoor Navigation (IPIN), 2010 International Conference on*, pages 1–6, 2010.
- [8] O. J. Woodman. An introduction to inertial navigation. *Technical Report Number 696*, 2007.